EXPERIMENTAL STUDY ON THE EFFECT OF SLAT TO AERODYNAMICS PERFOMANCE OF AN AIRFOIL

AZRI DINNIE BIN ROSLI

Report Projek Sarjana Muda

Supervisor : DR NAZRI BIN MD DAUD

Second Examiner : DR FADHLI BIN SYAHRIAL

Faculty of Mechanical Engineering

UNIVERSITI TEKNIKAL MALAYSIA MELAKA

2017

DECLARATION

I declare that this project report entitled “Experimental study on the effect of slat to aerodynamic performance of airfoil” is the result of my own work except as cited in the references

Signature :……………………………

Name :………………………………

Date :………………………………

.

SUPERVISOR'S DECLARATION

I have checked this report and this report can now be submitted to JK-PSM to be delivered back to supervisor and to second examiner

Signature :…………………………….

Name of supervisor :…………………………….

Date :…………………………….

DEDICATION

To my beloved mother and father

ABSTRACT

Slat to aerodynamic that effect the efficiency, performance and quality of aerodynamic system. The purpose of this study is to determine which slat have the effect to aerodynamic performance or not with compare the lift coefficient and drag coefficient of airfoil with has slat and the lift coefficient and drag coefficient of airfoil without slat. The angle of airfoil and slat are change for different type of experiment. The difference in lift and drag coefficient of airfoil with slat and airfoil without slat are being investigate. The results obtained from the measurement and analysis is compared of airfoil with slat and airfoil without slat. Airfoil with slat show more preferred result compare to airfoil without slat in term of lift and drag coefficient. Airfoil with slat show more high in lift coefficient compare to airfoil without slat. Overall, for airfoil with angle of slat -30^{o} (downward) and angle of attack of airfoil 20^{o} show the most preferable result because this experiment get the highest in lift coefficient and lowest in drag coefficient. Based on the results, recommendations and suggestions are made to improve the aerodynamic performance.

ABSTRAK

Kesan bidai terhadap kecekapan,prestasi, dan kualiti sistem aerodinamik. Tujuan kajian ini adalah untuk menentukan sama ada bidai memberi impak terhadap kecekapan aerodinamik atau tidak, dengan membandingkan pekali daya angkat dan seretan pekali aerofoil degan mempunyai bidai dan pekali daya angkat dan seretan pekali aerofoil tanpa bidai. Sudut aerofoil dan bidai diubah untuk belainan jenis eksperimen. Perbezaan dalam pekali daya angkat dan seretan pekali aerofoil dengan bidai dan aerofoil tanpa bidai akan disiasat. Keputusan yang diperolehi daripada pengukuran dan analisis dibandingkan aerofoil dengal bidai dan aerofoil tanpa bidai. Aerofoil dengan adanya bidai persembahkan hasil yang lebih diutamakan berbanding dengan aerofoil tanpa bidai dari segi pekali daya angkat dan pekali seretan. Aerofoil dengan bidai menunjukan lebih tinggi dalam pekali daya angkat bandingkan dengan aerofoil tanpa bidai. Secara keseluruhan, bagi lelayang dengan sudut bidai -30^{o} (ke bawah) dan sudut serang aerofoil 20^{o} menunjukkan hasil yang paling digemari disebabkan ujikaji in mendapat bacaan yang tinggi dalam pekali daya angkat dan bacaan rendah dalam pekali seretan.. Berdasarkan keputusan, cadangan dibuat untuk meningkatkan prestasi aerodinamik.

ACKNOWLEDGEMENT

First of all, I would like to express gratitude to my supervisor, Dr Nazri Bin Md Daud, who has helped me so much by constantly imparting his acknowledge and ideas so that I could complete my PSM project successfully. Sincere thanks to Dr. Fadhli Bin Syahrial for evaluating my final year project. The ideas and suggestions given were valuable for me to complete this project.

Beside that, I would also like to thank Faculty of Mechanical Engineering (FKM), Universiti Teknikal Malaysia Melaka (UTeM) for giving me this opportunity to complete this project and allowing me to utilize all the necessary equipment and tools needed for this study.

Finally, I would like to acknowledge with much appreciate to my family and friends for their continuous support and encouragement throughout the project period. \

TABLE OF CONTENTS

LIST OF TABLES

NO. TITLE

LIST OF FIGURE

LIST OF SYMBOL

CD	=	coefficient lift
CL	=	coefficient drag
P	=	pressure
ρ	=	density
T	=	temperature
HIV	=	high voltage cable
(^{0})	=	degree
mm	=	millimeter
Hz	=	Hertz
N	=	newton
T	=	temperature
^oC	=	degree celcius

CHAPTER 1

INTRODUCTION

1.1 BACKGROUND

An experimental investigation on the use of NACA 0015. Airfoil is the shape of wing or a structure with curved surface designed ad with aerodynamic shaped, in this experiment the airfoil is combine with slat, as shown in figure 1. The airfoil made from ABS (acrylonitrile butadiene styrene) filament, ABS filament is made from oil-based resources and has a much high melting point, it’s also hard and strong. The airfoil had a slat at leading edge. Slat actual is a narrow of plastic, slat ca change the shape of the wing when they are extended and allow the wing to produce more lift so that the airplane can fly relaxed.

The amount of lift generated by a wing depends on the shapes pf the airfoil. Slat are aerodynamic surface on the lading. This experiment is to test either the slat has an effect to aerodynamic performance of airfoil.3. lift force that directly opposes the weight of an aerodynamic object and holds the airplane in the air which it is positive force. Lift force only exist if has motion. No motion, no lift.

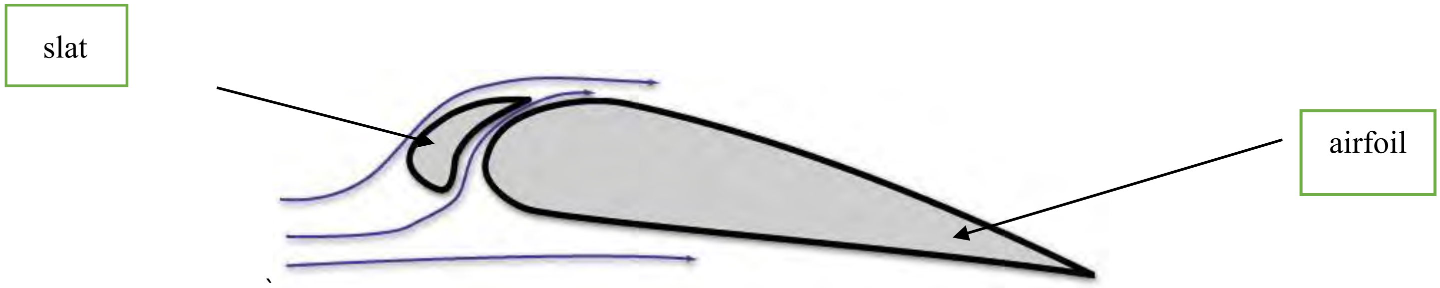

Figure 1 : airfoil with slat

1.2 PROBLEM STATEMENT

Many researchers have studied the airfoil for separation control of airfoil without slat. Most of their studies were focused on an airfoil in various applications. Since, there is a lack of study in determine drag and lift coefficient for the airfoil with has slat on it. Compare drag and lift coefficient by using different angle of attack and different angle of slat. Slat allow the airplane generate more lift and reduce the power usage of airplane, nowadays the airplane use extra power on the engine because the drag force and need to use more fuel.

1.3 OBJECTIVE

The objectives of this project are as follow:

- Measure the effect of angle-attack on slat and airfoil
- Study the effect of leading edge slat on lift and drag coefficients
- Compare the result of application of slat to the one with no slat

1.4 SCOPE OF PROJECT

The scope of this project are:

- Design and material of airfoil
- 9m/s air velocity
- Measure CL and CD

1.5 General methodology

The action that need to be carry out to achieve the objectives in this project are shown:

1. Literature review
    - Journals, article, book or any materials regarding the project will be review.

2. Inspection
    - The velocity profile will be determined and discuss with the supervisor.

3. Measurement
    - The measurement will conduct at a lab. For airfoil test will be conducted inside wind tunnel. The venue of test is still in discussion with supervisor due to insufficient equipment used to conduct the test. Measurement data of lift and drag force will be collected and compare with the different usage of slat angle and airfoil angle.

4. Analysis and proposed solution

   - Analysis will be present on how slat effect on lift and drag coefficient velocity of wind and the angle of attack will help in creating vortex near the surface as well as the different angle of airfoil need to be determining to lift and drag coefficient. Solution will be proposed base on analysis.

5. Report writing

   - A report on this study will be write at the end of the project.

Chapter 2

LITERATURE REVIEW

2.1 overview

Literature review is focused on previous study in the related field to obtain knowledge and information for the present study. In this chapter, journal and technical reports from other researchers are selected to be reviewed. The results obtained from the previous study will be compared.

2.2 Experimental instigation on the, effect of slat geometrical configuration on aerodynamic noise

The present study have addressed the slat noise on slat, deflection angle and overlap although slat noise level and ghostlike content are subject of increasing concern in aeronautic engineering. The paper show new experimental data on the topics. A selection of microphones placed in a closed-section wind tunnel was use in the experiment. Beam forming signal processing enhanced by DAMAS (Deconvolution Ap- proach for the Mapping of Acoustic Sources) was useful to the data. The investigational data covered a range of angles of attack and Mach numbers, for which the characteristic slat noise signature features high-level narrow-band peaks, broadband noise and a single broad tone. The narrow-band peaks frequently dominate the slat noise ranges and arise at Strophe numbers up to approximately 5. The broadband noise is well branded for Strophe numbers between 5 and 20, whereas the broad tone arises for Strophe above 20. A total of 10 dissimilar slat configurations, including variations in slat, overlap and deflection angle were verified. The slat noise dependence on slat, overlap and slat deflection angle was measured by letting each of them vary distinctly.

2.2.1 Methodology

This running process of experiment begins with aerodynamic and aeroacoustic measurement were conduct in close circuit wind tunnel. The test section was 1.3 m high, 1.7 m wide and 3.0 m long. The reduction ratio was 1:8 and the flow was determined by an eight blade axial fan. Then, do a pressure measurement and instrumentation , The wing was instrumented for chord-wise static pressure measurements at the middle span with a single line of 143 pressure tappings as shown in figure 2

Figure 2 : schematic view of the 143 pressure tappings

Next design the array and acoustic instrumentation, An array composed of 62 1/4-inch repolarized pressure microphones. The array, intended as an optimized Archimedean single-arm twisting. Then do a Geometrical sets of the high-lift model.

2.2.2 Result and discussion

- Effect of slat setting on the mean surface pressure distributions.

The result of the circulations of a forward positioned element is to reduce the flow acceleration over the suction side close to leading edge of element, there are 2 results from a downstream lifting element, for example the main element relative to the slat. They are called 'circulation effect' and 'dumping effect'.

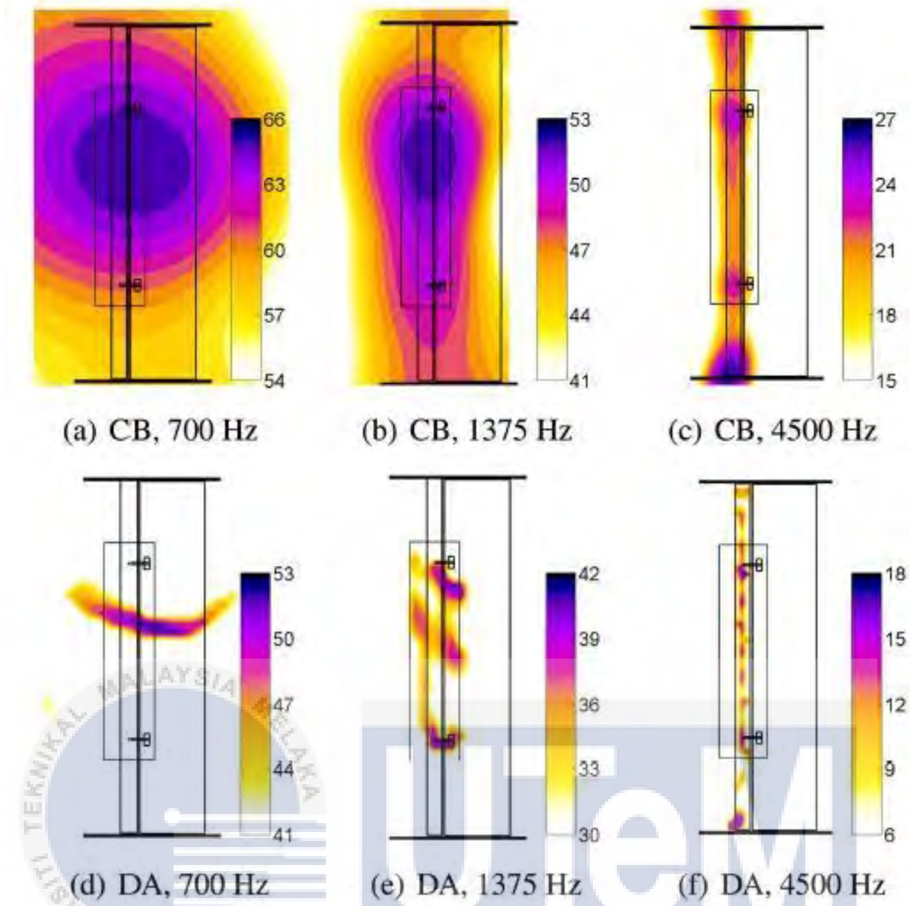

Figure 3 : conventional beamforming (a,b and c) / DAMAS (d,e and f)

The 'circulation effect' is related to the up wash in the trailing-edge region of the slats reason by the circulation on the main element and promote a rise in the circulation of the slat for the kutta (principle in steady-flow fluid dynamics) condition to gratified.

2.2.3 conclusion

In conclusion for a huge portion of the parameter range investigated, the small frequency multiple narrow band peaks are the supreme silent feature of the slat noise. I overall, such a noise component reduces as the angle of attack and gap increase. The data are limited, on the other hand, they suggest the gap result on the slat noise may be powerfully dependent on the overlap configuration, meanwhile the increase in the narrow band peaks with a gap reduction.

2.3 Transient phenomena in separation control over a NACA 0015 airfoil

The article show transient phenomena occurring during the impulsive control of flow separation over a NACA 0015 airfoil at an incidence angle of and a chord Reynolds number of 1 million. Actuation is did via pneumatic vortex generators, impulsively triggered in order to examine the transient phenomena corresponding to the attachment procedure and, conversely, to transient re-separation happening when the actuators are switched off. Capacities are performed using a linear array of tottering pressure transducers and an only traversing crosswire.

2.3.1 Methodology

The experiment run in the wind tunnel with test section size of 2.4 meter by 2.6 meter, with a velocity of air 40 meter per second. Naca0015 with chord length 0.35m and span with length 2.4m. airfoil pitched at an incidence 11°. This Angle-of-Attack corresponds to a 2D separation occurring 30% of chord up stream of the trailing edge. The stream wise coordinate, *x* is defined from the tailing edge (TE), *x A* corresponds to the distance from the leading edge (LE); *y* is normal to the wind tunnel axis, *z* being the span wise way. Time is non dimension allied with the length of the separation, T + = tU ∞ / L sep , where U ∞ is the external velocity and L sep = 1/3c is the length of the separated area. A limited series of smoke visualizations have been performed on a larger NACA 0015 profile still at AoA of 11 °in a small speed visualization wind tunnel.

2.3.2 Results and discussion

The mean velocity profiles measured at x/c = 1 are given on figure 4. for both natural and controlled steady cases. Several span- wise positions have been measured in order to evaluate the 2D character of the flow, either for separated or fully attached. The 2D character of the flow is observed. As expected, the wake thickness reduces by approximately 40%, evolving from 0.053c to 0.0316c for natural and steady attached cases respectively. The Reynolds shear stress (< u' v' >) distributions are shown in figure 5 . The turbulent energy of the uncontrolled case is ~40% higher as compared to the controlled case.

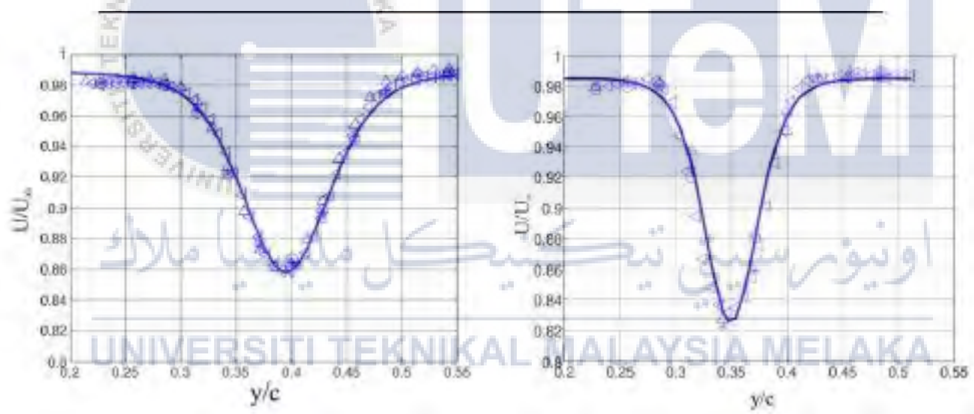

Figure 4 : mea velocity profiles. a) uncontrolled, seperated case b) controlled, attached steady case

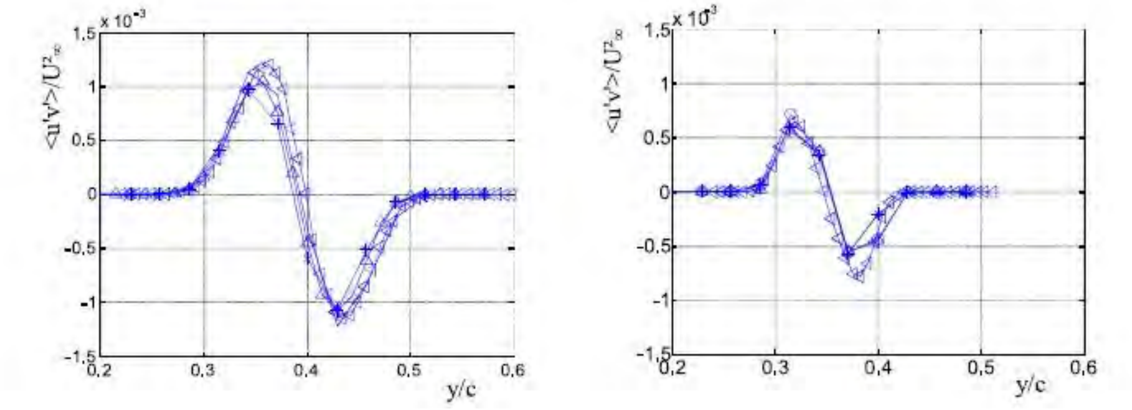

Figure 5 : shear stress velocity profiles.   a) uncontrolled, seperated case b) controlled, attached steady case

2.3.3 conclusion

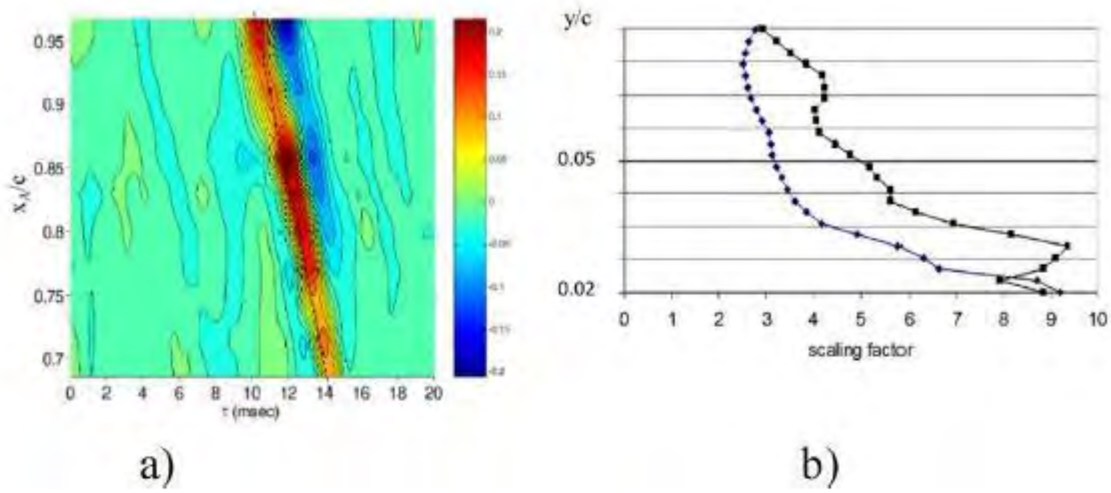

Figure 6

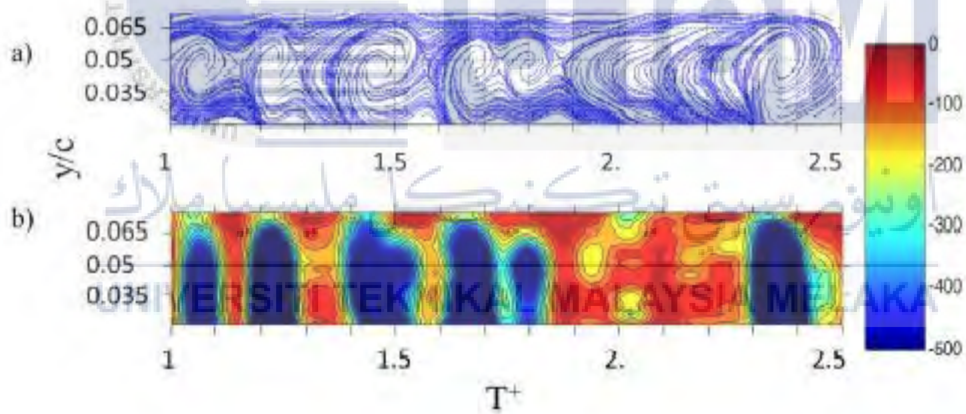

Figure 7

Figure 6 (a) show the result if contour map of the pressure ad velocity correlation , figure 6(b) show scaling factor apply to the estimated u and v velocity from pressure signal. Figure 7 show the time evolution of the flow field over the airfoil, 7(a) is in plane streamline, 7(b) is vorticity contours.

2.4 Investigation of slat heel effect on the flow field over multi-element aerofoils

This journal present the results obtained from an experimental an study of the flow field over a multi element airfoil includes either a conventional or an advanced slats. Details dimension of the mean flow and turbulent quantities over a multi element airfoil model with also type of slat have been made in wind tunnel using fixed and flying hot wire. Have 2 angle fo attack of slat, 10 and 20 degree. The benefit of the advanced slat was more marked for the multi element aerofoil placed at the higher angle of attack.

2.4.1 methodology

The experiment conduct in wind tunnel with low speed of **wind** velocity**. The tunnel** having 600x600 mm^2 cross section. The model configuration spans the test section made with NACA 4412 as shown in figure 8. The main investigational technique for the present research was a flying hot-wire (FHW) mounted on a precise computer controlled mechanism. The method is based on moving the investigation along a set path, in our case a bean formed curve with a big enough velocity to avoid hot-wire signal rectification associated with fixed hot wire reviews in reversing flow. The calculation were obtain from a number of points on the lower part of the probe curve path during single sweep, and for the study of the act of the slats. 20 evenly space points were selected for complete analysis. Each sweep was repeated 200 time. The installation of the multi-element aerofoil in the wind tunnel, and the principle of the mechanical implementation for the bean shaped curve path use is illustrated in Figure. 9.

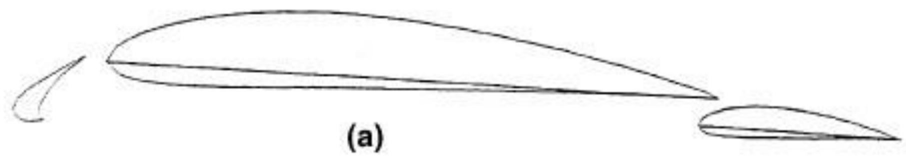

Figure 8 : NACA 4412

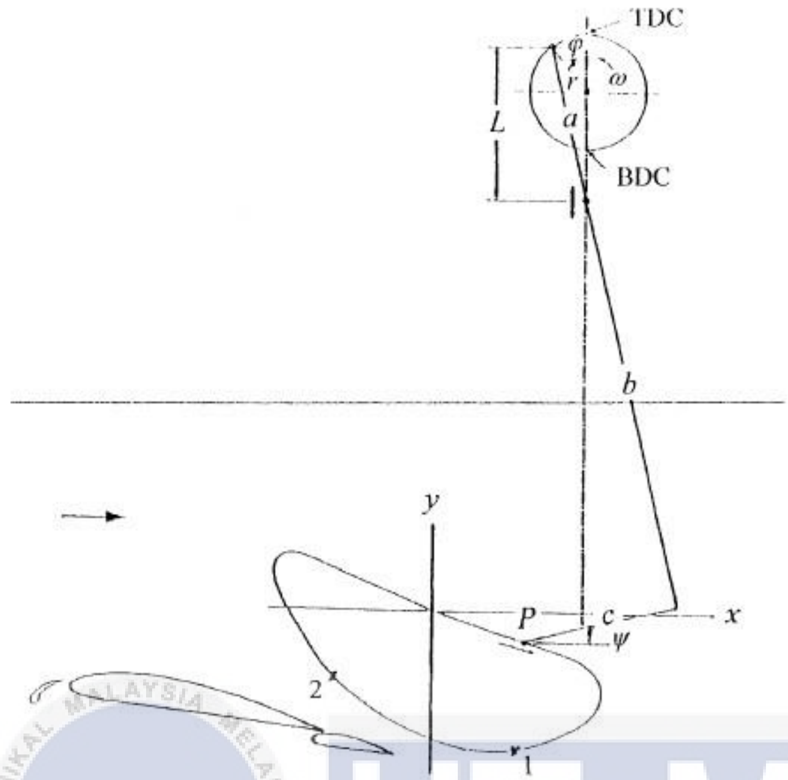

Figure 9 : Four-bar FHW mechanism, notation and wind tunnel measurement

2.4.2 Results and discussion

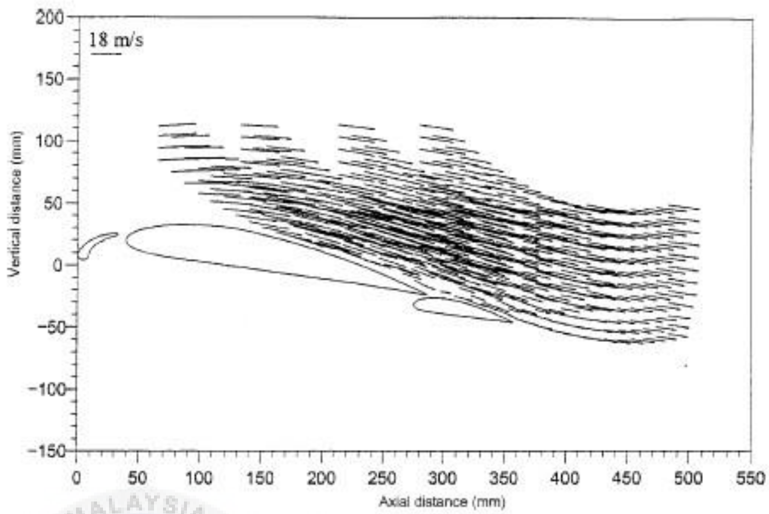

Figure 10 : mean velocity vector with advance slat

The velocity vector indicate that the flow is attached to the model surface and there is no sign of separation. An accelerated flow over the front of the main airfoil is guilty for making suction and lift. Figure 10 show the mean vector velocity results.

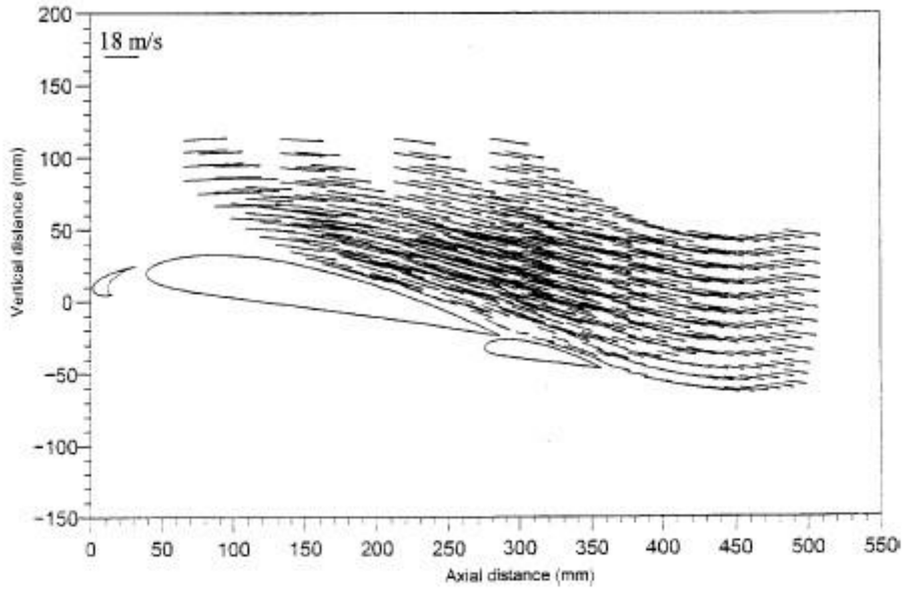

Figure 11 : mean velocity vector with conventional slat

Figure 11 show the mean velocity vector with conventional slat. These demonstrate similar velocity fields for the two slat design, the flap where the advanced slat case exhibits velocities up to 1 m/s higher than for the corresponding conventional slat case. This demonstrates a better performance for the advanced slat.

2.4.3 Conclusion

Lift and high device are crucial for the safe and economical operation of aircraft. This experiment has investigate the performance of an advance and conventional slat. Comparing the related flow fields, the multi element airfoil equipped with the advanced slat had a superior act in terms of both an advanced mean velocity field and lower turbulent Reynolds stresses in particular near the rear of the main aerofoil. The result for slat showed worsening in the flow field from attached (advanced slat) to intermittent parting (conventional slat) at the rear part of the main aerofoil. This designates that stall for the three element airfoil equipped with the conventional slat will happen at a lower angle compare with the consistent stall angle for the three element aerofoil with an advanced slat.

2.5 Effect of an excrescence in the slat cover: flow field, acoustic radiation and coherent structure

The current experimental study is to explore the mechanism of slat noise generation. The noise of slat during aircraft is already a barrier to the development of quieter commercial airplane. Most of the published works related to slat noise reflect clean idealized geometries, while real slat contain certain imperfection to allow its operation. The effect of a protrusion on the slat cavity surface on the unsteady flow round the slat and on the propagated sound was here investigated via numerical simulation. The protrusion model a sealing device designed to avoid metal–metal contact. The effect of the seal on the time averaged pressure distribution is narrow to the region close to it. Though, tonal peak in the noise emitted from the slat region are significantly higher once the seal is introduced. The present results show that, at the frequency of one of the tonal peak, pressure fluctuations outside the cove are highly connected with large scale structures in the cove mixing layer and at its impingement on the slat lower surface. The result also show that the outline of the seal increase the coherence of these structure.

2.5.1 methodology

The simulation of a high lift airfoil. The present simulation use the MD 30P30N as base line geometry. The high lift airfoil has been extensively study NASA. The geometry parameter of slat is 30 degree of deflection , 2.95% gap and -2.5% overhang. And the geometry parameter of flat is 30 degree of deflection, 1.27% gap and 0.25% overhang. The simulations described in this paper are computed using the commercial code Power FLOW 4.3a. This code is based on the Lattice-Boltzmann method (LBM). The Proper Orthogonal Decomposition (POD) is a correlation technique that delivers a basis of orthogonal function $\{\varphi k\}$, re-ferred to as POD functions or mode, that optimally rot a set of first data $\{\mathbf{q}k\}$. The meaning of optimality is that the POD basis minimize the quadratic error under a given inner product between the variable consider. It mean that the average projection of the flow realizations on the POD basis must be maximize. The maximization lead to the eigenvalue problem

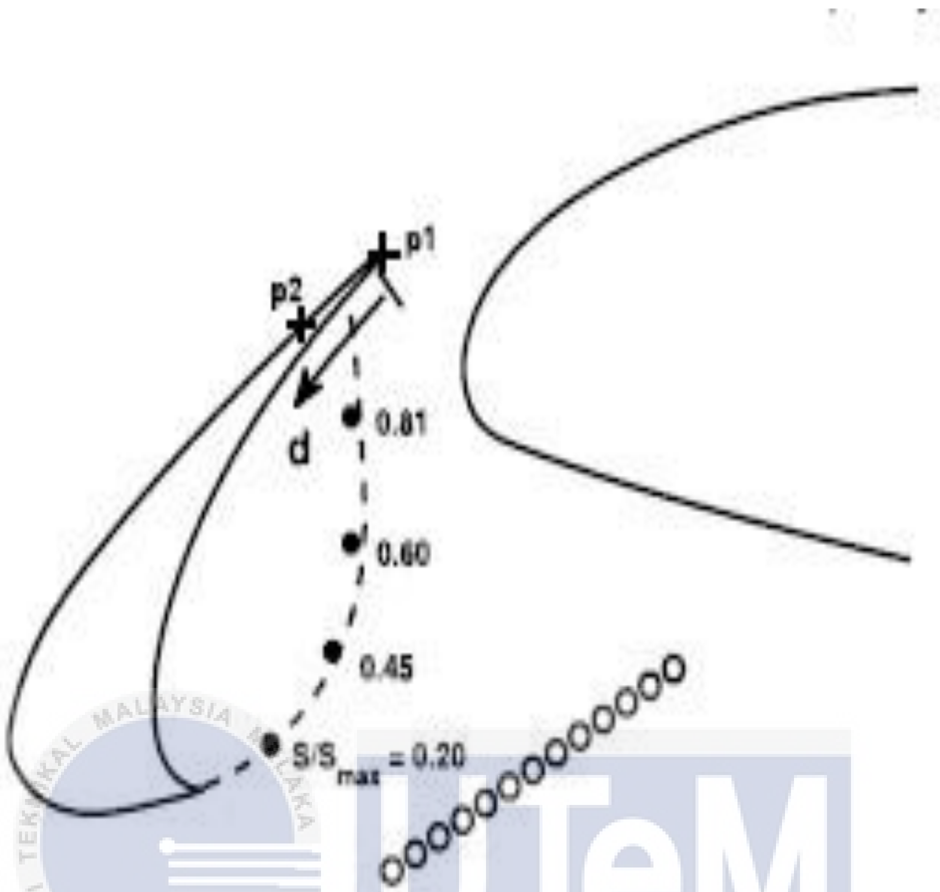

Figure 12

Figure 12 show the Scheme of the slat region. Definition of probes at slat trailing edge and suction side and four probes close to the arc defining the location of the mean mixing-layer (defined by the dashed line). Represents the distance from the cusp along the mixing layer and *Smax*refers to the length of the entire mixing layer path from the cusp towards the reattachment point. Also indicating the coordinate that defines the position of the seal. The open circle show the location where A (x, y) is non zero in the _**q***j*, **q***i*_*pff*inner product.

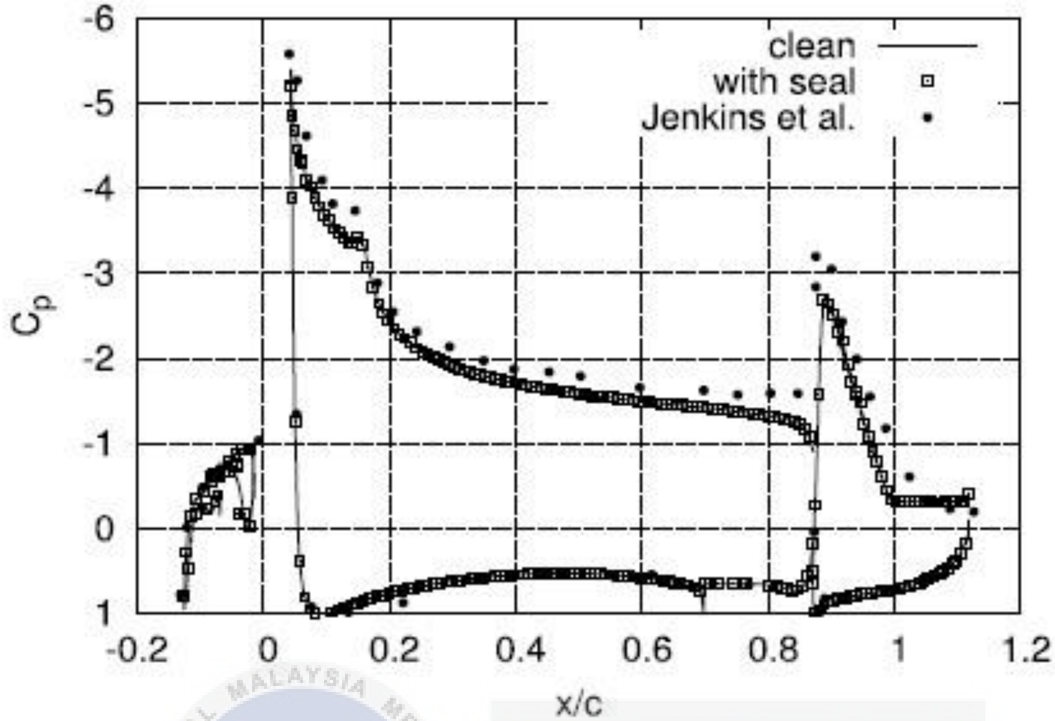

Figure 13

Figure 12 show the average time pressure coefficient distribution along the surface of the airfoil.

2.5.2 Result and discussion

Figure 14 : average time streamline in cove region

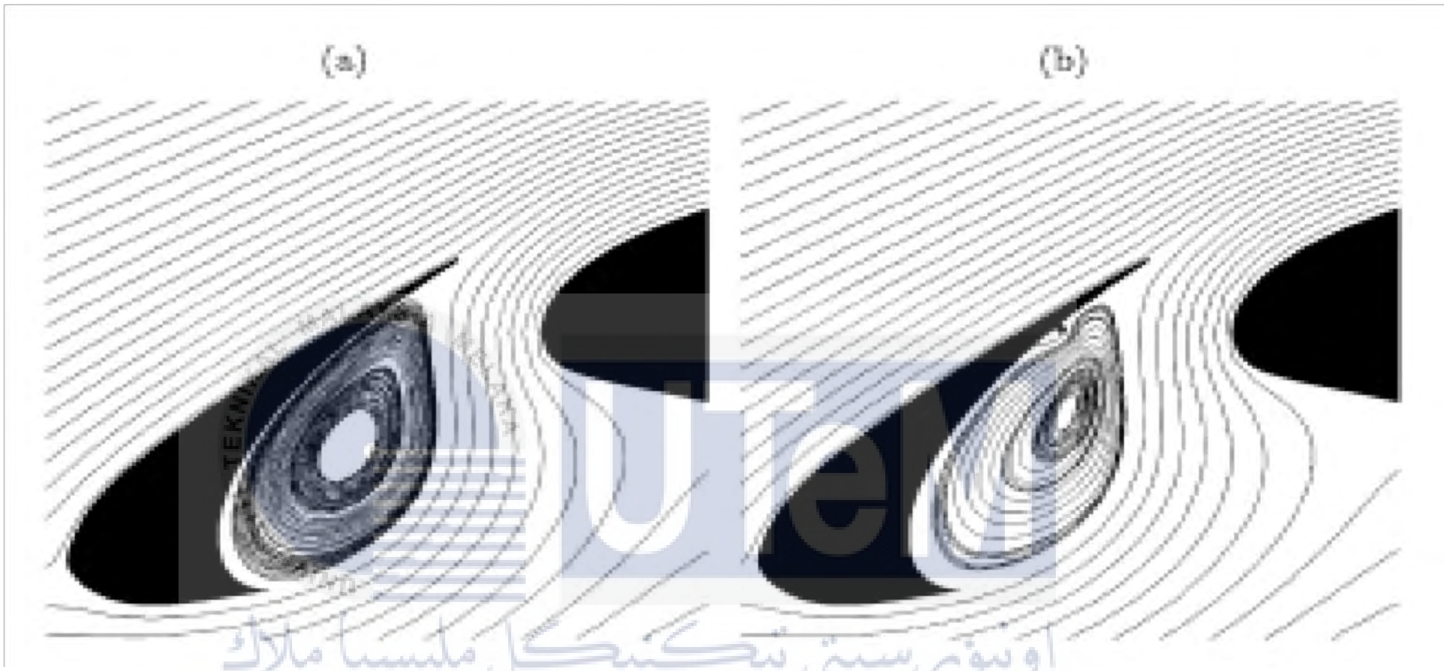

Figure 13 shows the time-averaged streamlines in the central sec-tion of the slat cove region. Despite the presence of the seal in figure (b), the averaged flow characteristics are similar to the clean configuration. As the mixing layer reattaches, part of the flow is pumped through the slat gap and part of it is directed towards the seal, stream over it and recirculate trapped confidential the cove. Nevertheless the seal causes translation of the center of recirculation. The nondimensional Turbulent Kinetic Energy in the central section is shown in Figure 14 . The contour are in logarithmic scale and in both cases represent the same levels. It is clear that the presence of the seal reduces considerably the intensity of the fluctuations confidential the recirculation zone. On the other hand the configuration with the seal exhibits significantly extra intense TKE levels close to the mean mixing layer reattachment point.

2.5.3 conclusion

Finally, to conclude, the present work showed that. The configuration considered were based on the high-lift airfoil MD 30P30N and the included element modeled a seal located on the slat cove surface to avoid metal contact in cruise configuration. The effect of the seal in the averaged pressure distribution is mini-mal. The seal changes the center of the time-averaged recirculating zone inside the slat cove and reduces the amount of vortical structures entrapped that reach the early stages of development of the Kelvin Helmholtz vortices in the mixing layer. As a con-sequence, these span wise vortices remain almost two dimensional for a longer distance from the cusp. In the spectra of near field and acoustic fluctuations, the amplitude of the distinct low-frequency tonal peaks are-increased with the introduction of the seal. Proper Orthogonal Decomposition was used to study the effect of the seal in the coherent structures inside the slat cove: analysis of the leading POD modes at the frequency of one of these peaks reveals that the seal increases the coherence of structures associated with the mixing layer, and that these vortical structures are highly correlated to pressure fluctuations radiating from the airfoil pressure side.

2.6 Failure mechanism analysis and reliability assessment of an aircraft slat

The aim of this project is to investigate the failure mechanism analysis and reliability assessment of the slat. Firstly, based on the work principle, FTA (failure tree analysis) and FMEA (failure modes and effect analysis) are used to analyze the potential failure modes and mechanism of failure modes. Secondly, simulation model Is established using LMS Virtual Lab and it is validated based on test data and-mathematic model. Lastly, the reliability and failure cases are assessed founded on the result of dynamic simulation. The reliability analysis results show that transmission shaft fracture and motion seizure are the-main failure modes. Failure assessment show that the safety margin decreases to a very low value if transmission shaft fracture occurs, while a-roller seized can lead to slat motion-seizure.

2.6.1 Methodology

Firstly do a slat modelling and validation, build slat with simulation model. Preparing the model, rigid model building, and finite element model (FEM) building and craig-bampton mode calculation, do a rigid-flex coupling model building, hydraulic model and unites model building and parametric model building. All 6-step show of modelling show in figure 15.

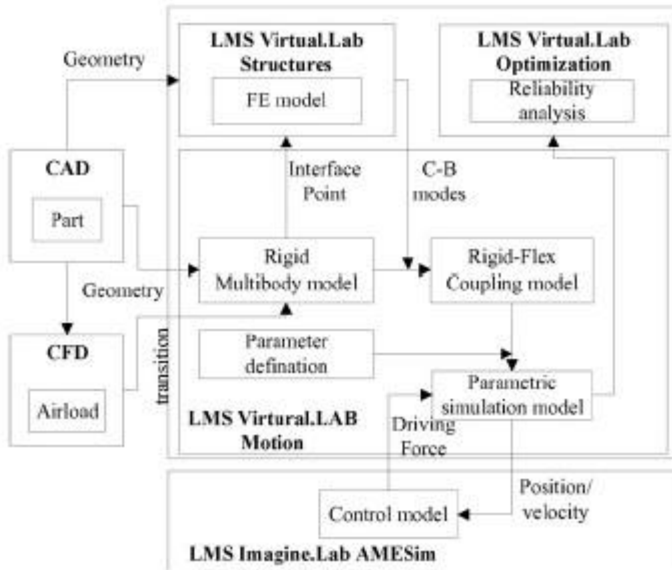

Figure 15: methodology modelling

Next step do a mathematical model of the slat. Calculate the reaction force analysis between support and track, calculate drag moment analysis during motion, calculate performance parameter analysis, and calculate coupling effect analysis of slat torsion and bending deformation. After all the calculation done, simulation model validation is the next step. Do a validation of the deterministic simulation model based on slat test, influence factors validation of simulation model based on mathematical model.

The reliability analysis and failure assessment base on dynamical analysis is the last method. Reliability assessment based RSM and MC.

2.6.2 Result

Figure 16 show the result of simulation model of slat. While figure 17 shoe the comparison of dynamic result. The result of parameter study is show in figure 18.

Figure 16: slat simulation model

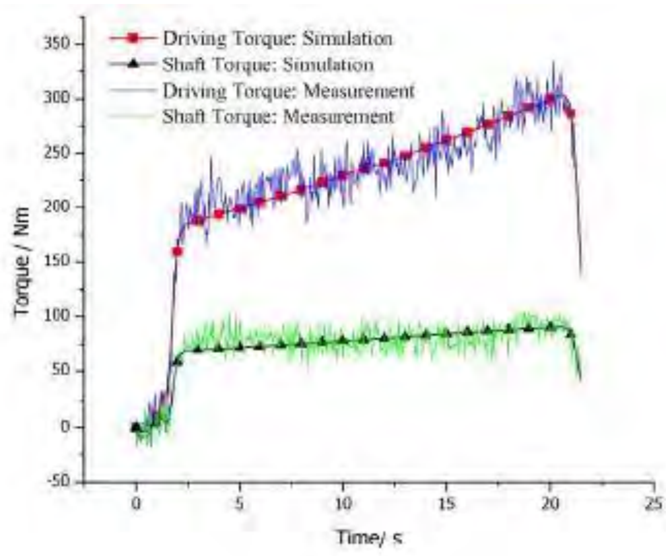

Figure 17: comparison of dynamic result

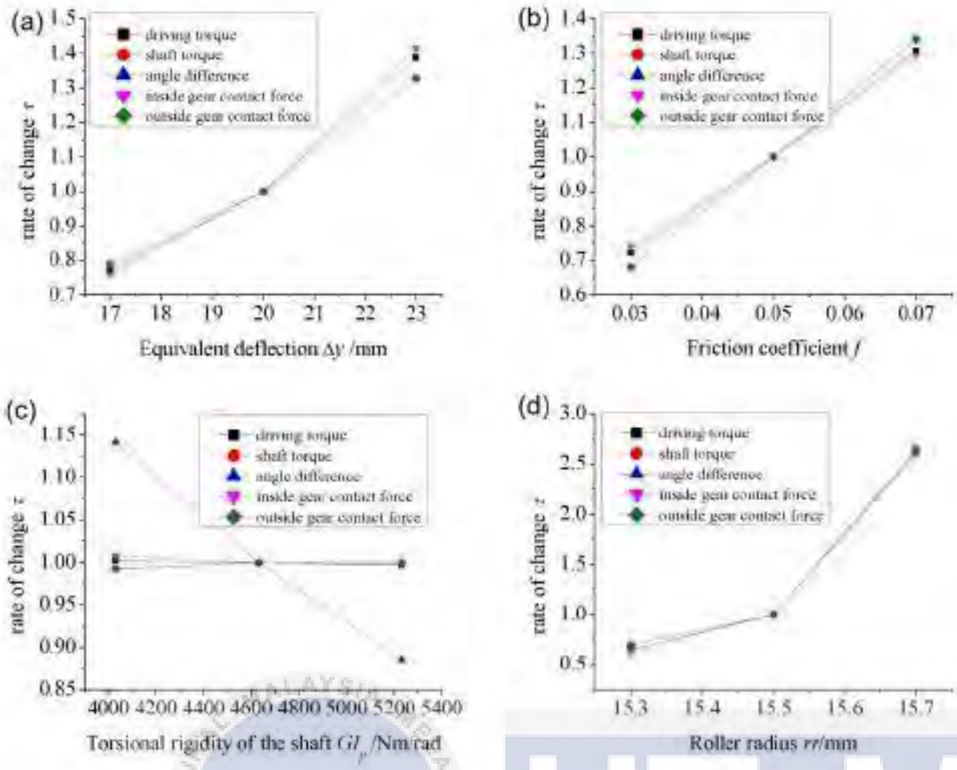

Figure 18: result of parameter study

2.6.3 Conclusion

The present study focuses on the failure mechanism analysis and reliability assessment of the slat mechanism. Failure modes and failure mechanism are fully analyzed, an simulation model, which is validated by test and mathematic model is used to analyze the reliability problems. The significant conclusions are:

1) Reliability analysis result show that transmission shaft fracture and motion seizure are the main failure modes, so it is necessary to monitor the driving torque and shaft torque.

2) Failure valuation shows that the safety margin decreases to a very low value if transmission shaft fracture occurs, while roller seized can lead to slat motion seizure. The advantage of the study is that failure modes and failure mechanism are fully discussed. What's more, deformation of the wing is considered during-slat modeling; the boundary condition is more close to the actual and the result are more accurate. However, a single slat is studied currently and the correlation between the slats has been-ignored. In addition, gust has not been considered. In the future, in order to obtain more accurate results of the-slats system, the model still needs to be improved.

Chapter 3

METHODOLOGY

3.1 Overview

This section will focus on the design of airfoil and the effect of the application on the slat at the leading edge of airfoil. The design and shape of airfoil is NACA 0015. The methodology is cover from the beginning of the research which is studies on previous research until the end data collection from the experiment,

3.2 Introduction

From the studies of the previous research, we can roughly conclude that the application of the slat can alter few parameters of the flow around the airfoil such as the pressure distribution and the velocity profile. To prove the early conclusion, a further research should be conducted. There will be few main stages in this research which are the preparation of the airfoil NACA0015, setting up the apparatus in the wind tunnel, conducting the experiment and collecting the data.

3.3 flow chart

Flow chart in figure 3.1 showed the flow of the methodology process of whole experiment in briefly by step by step.

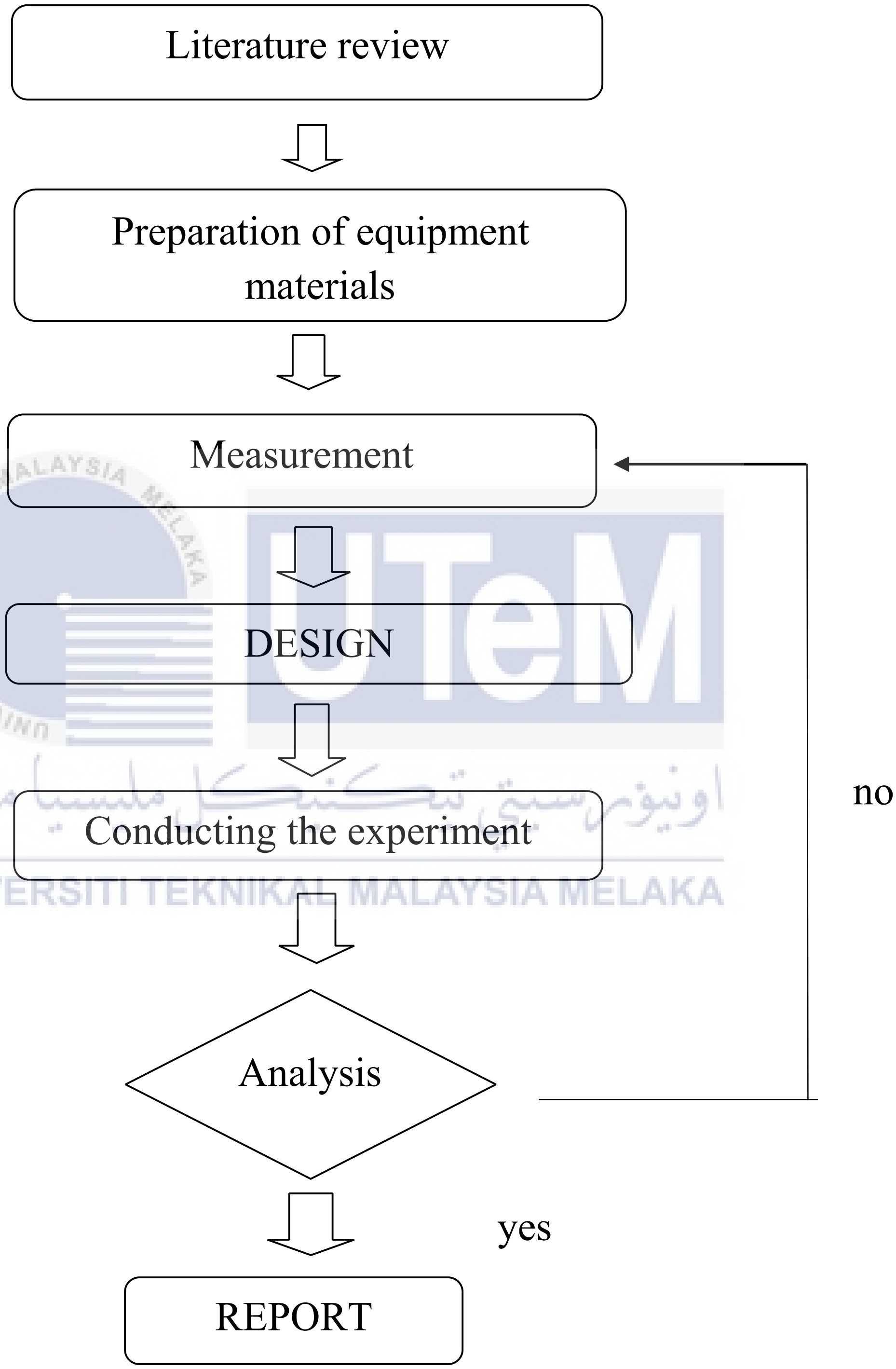

Figure 3.1 : flow chat

3.4 Equipment and Materials

The experiment was conducted at the lab by using airfoil as configuration. The airfoil will put in the wind turbine. And the air will flow through the airfoil to find the lift and drag of airfoil then calculate to find CL and CD. The materials used in experiment are listed as below. Before the experiment run, need to design the airfoil by using solidwork 2016 software. a) clay

b) Wind tunnel

c) Filament (ABS)

d) 3D printer

3.4.1 clay

Figure 19 : clay

Clay is a fine grained natural soil material that combines one or more core clay minerals with traces of metal oxides and organic matter. Clay is use in this experiment to connect the airfoil to the slat.

3.4.2 wind tunnel

Figure 20

Wind tunnel is tool used to test the aerodynamic research to study the effect of air moving past solid object. This wind tunnel place in fasa B. we will use this wind tunnel to test the drag and lift of airfoil.

3.4.3 filament abs

Figure 21

ABS (acrylonitrile-butadiene strene) is an oil based plastic, it is tough material that can be used to create robust plastic objects. This material is to create the airfoil. ABS is choose in this experiment because it more susceptible to typical 3D printing problem. Its strength, flexibility, machinability, and higher temperature resistance make it often a preferred plastic for engineers, and professional applications. This filament will put in the 3d printer. **3.4.4 3D printer**

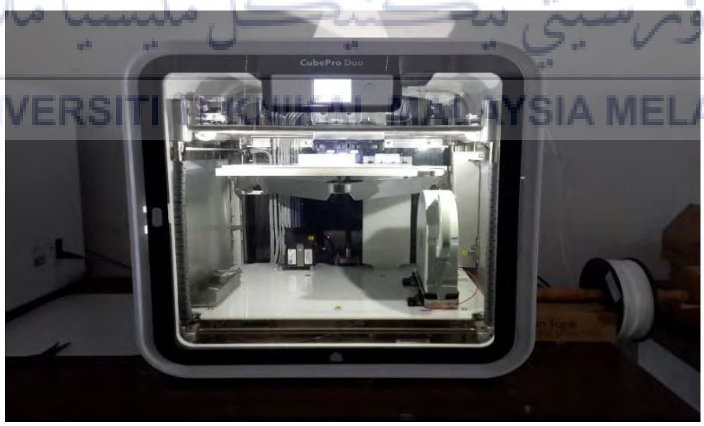

Figure 22

3D printer is machine to create the 3 dimension solid object from a digital file. This 3d printer is locate as fasa B UTeM. we use this 3D printer to create airfoil and slat from solidwork file that design before.

3.5 Design the airfoil

The design of airfoil is build using the software name by SOLIDWORK 2016 edition SolidWorks (stylized as SOLIDWORKS) is a solid modeling computer-aided design (CAD) and computer aided engineering (CAE) computer program that runs on Microsoft Windows. SolidWorks is published by Dassault System. The design is in 3 dimension. The shape of NACA airfoil is describe using series of digits. The NACA airfoil that will be used in this research is NACA 0015 airfoils. The NACA 0015 have they own coordinate and aspect ratio of airfoil. the measurement of NACA 0015 can be find at the website airfoiltools.com. Figure 20 show the NACA 0015 coordinate given in airfoiltools.com. website. After select the NACA coordinate or ratio, it's time to open the solidwork software to draw the airfoil with measurement given by that website. The dimension of the airfoil are 130mm of chord and 130 of span length, the length of slat is 20mm and 9mm hight. Figure 20,21 and 22 is the design made by solidwork software.

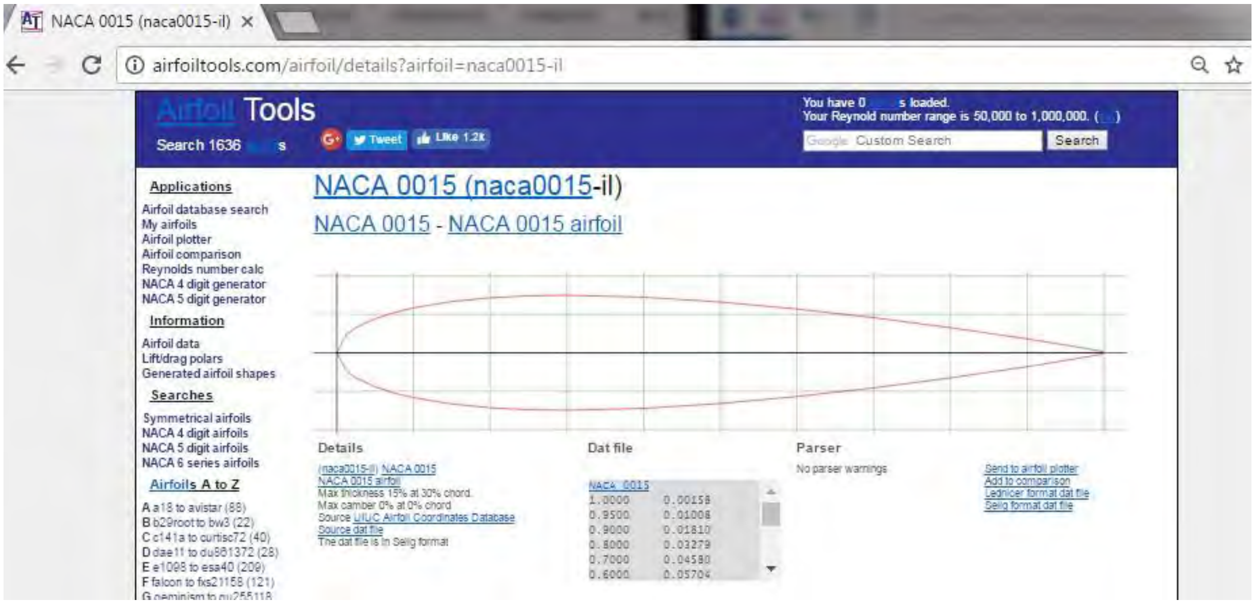

Figure 23: naca 0015 coordinate in the website

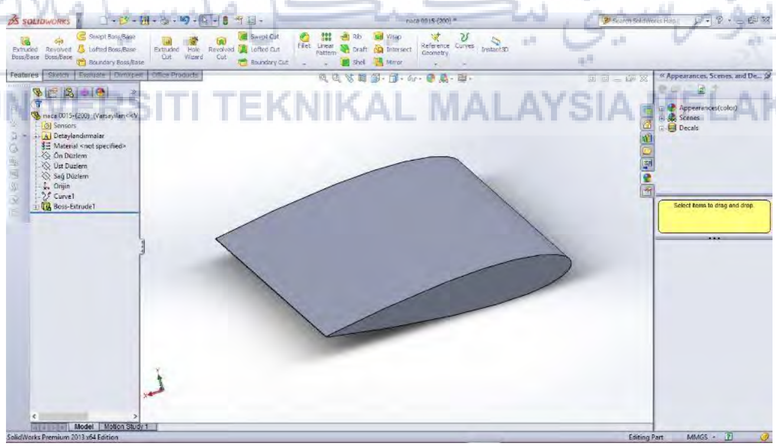

Figure 24 : NACA 0015 design in solid work

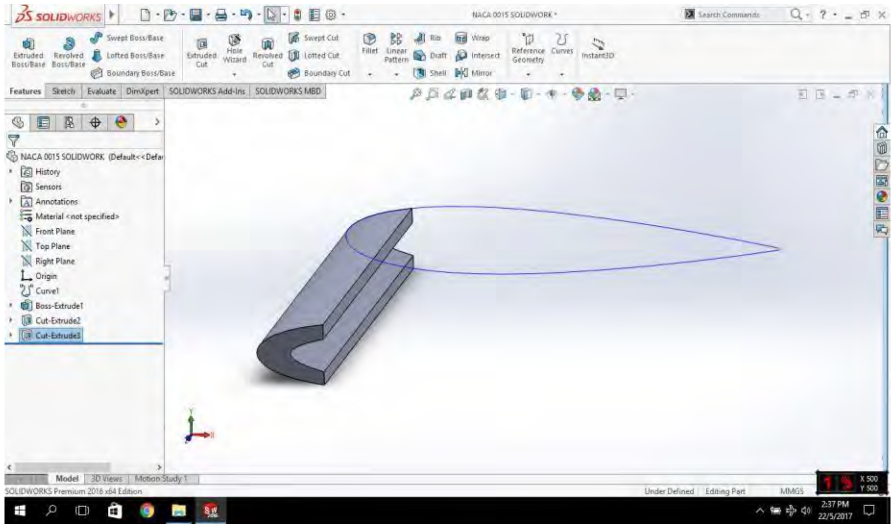

Figure 25: slat of naca 0015

After design the NACA 0015 airfoil is done, the next process is printing the design made before, by using machine name ‘CubePro Duo 3D’ as show in figure. Before that we must inside the design we made into the computer that connect to the printing machine. Then we can choose the density of airfoil to print, and we select ‘almost full’ for that print design. Before print we must convert the solidwork save file to STL file. Figure 26 show the 3d printer machine to create the airfoil NACA 0015.

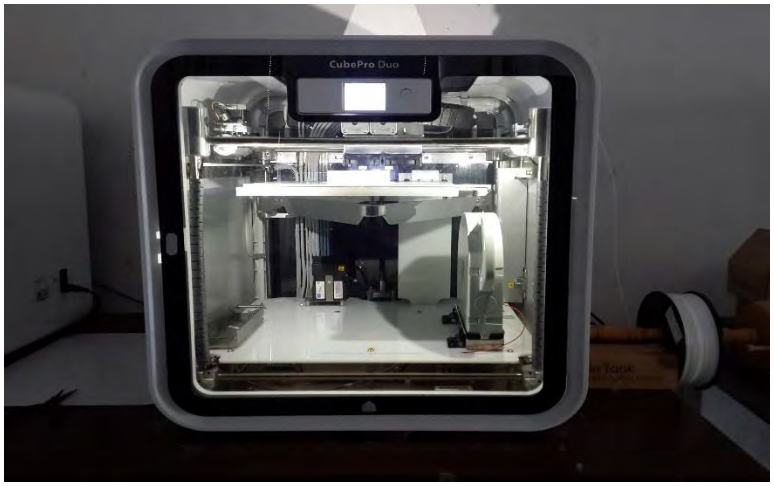

Figure 26: CubePro Duo 3D printer

It take almost 6hour to build the airfoil and 2hour to build slat by that machine. We use ABS filament as the material of airfoil. Figure 27 show the airfoil and slat of airfoil after print. To connect the airfoil to the wind tunnel must make a hole at side of the airfoil and put screw in the hole.

Figure 27: NACA and slat

3.6 Conducting Experiment

The experiment was conducted by run the experiment with different in angle of attack and angle of slat. This project running at the lab at kompleks kejuruteraan mekanikal (fasa B). the experiment will conduct by using subsonic wind tunnel brand ESSOM with model of MP130D place in fasa B at turbo machinery lab. Before run the experiment Encik Faizal as assistant engineering in charge for the turbo machinery lab will teach us how to conduct the wind tunnel. To run the experiment is quiet simple and not to complicated. Firstly the test here will take place with using only NACA 0015 without slat as a base case.

Figure 28 : NACA and slat (+30° angle of slat)

Figure 28 show the NACA and slat already connect by using clay. Draw the line on side of the airfoil and slat for easy to measure the angle of slat (30 degree upward and 30 degree downward).

Figure 29 : NACA inside the wind tunnel

Then, put airfoil to the rod inside with tunnel connect the screw made before. The leading of airfoil must face to the wind some from. Next step is plug in the plug for the power supply. The wind tunnel can be run. In this wind tunnel system, the only thing that can be controlled directly by the user is the speed control module.

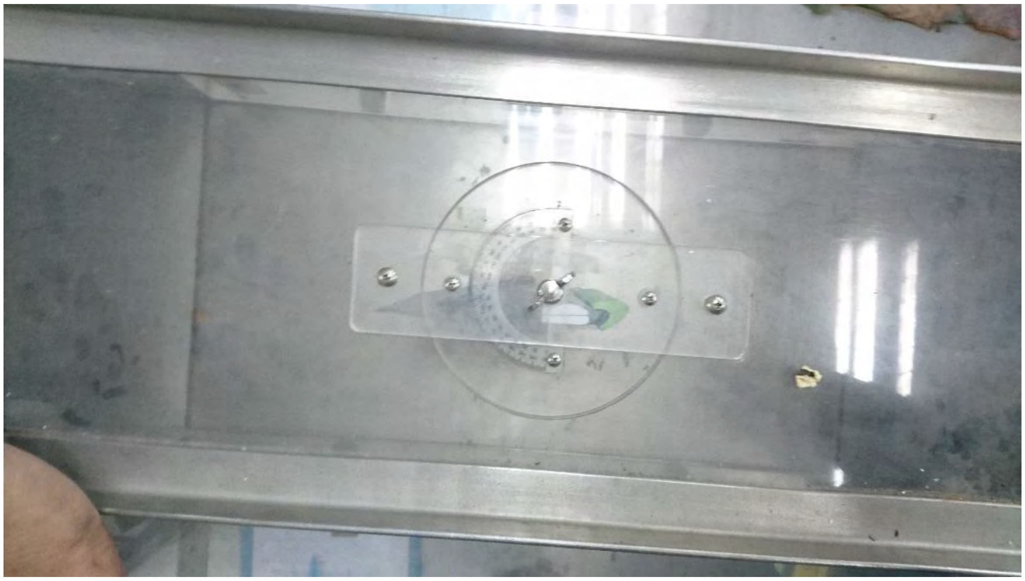

Figure 30 : protractor at top of wind tunnel

Protractor at top of wind tunnel to see whether the airfoil is straight or not. And to alter the angle of attack of airfoil, as show in figure 30.

Figure 31 : slope lever of pressure water

Figure 32: speed control module

This speed module control allow user to control three parameters which is the frequency, voltage and the current. We change the frequency to alter the velocity of the air. When we increase the number shown in the panel, and the parameter is selected at the frequency, the height of water at the slope will increase. The height of water increase will be measured in mm and then we have to refer to the chart provided to determine the velocity of the air as show in figure 31. We set the frequency to 15.00 Hz as show in figure 32 .When referring to the chart, we have the velocity of air of 9.5m/s.

3.7 Data Collection

In this experiment, only the drag and lift force ca be obtained from the indicator module. For the drag and lift coefficient must calculate by it safe from the drag and lift force obtained before. For the base case (airfoil without slip) which is NACA 0015 airfoil, a simpler table because it only dealing with angle of attack and the forces only and one table is enough to tabulate the data show (Table 3.7.1). for the experiment involving the airfoil with the leading edge slat, more table is required. A lot of experiment will be conducted as this airfoil has more changeable parameters and this will make 3 combinations of airfoil with different angle of slat (Table 3.7.2).

Angle of attack (°)	Lift Force (N)			Drag Force (N)		
	Initial	Final	Actual	Initial	Final	Actual
0						
5						
10						
15						
20						

Table 3.7.1: table use for base case in experiment

Angle of slat (°)	Angle of attack (°)	Lift force (N)			Drag force (N)		
		Initial	Final	Actual	Initial	Final	Actual
	0						
	5						
	10						
	15						
	20						

Table 3.7.2: table use for slat and airfoil experiment

CHAPTER 4

RESULTS AND DISCUSSION

4.1 Overview

In this study, the data and results of drag force, lift force, drag coefficient, and lift coefficient of airfoil from the experiment. The data and results obtain during the experiment will be represented in a quantitative value and it is all tabulated. The velocity used is 9.5m/s. The result will be in two parts:

1. The results for the base case (NACA 0015 airfoil without slat)
2. The results for the NACA 0015 airfoil with slat.

4.2 Experimental Results

Experiment 1 was conducted by using only base case of airfoil with 5 different angle of attack is 0°,5°,10°,15°,and 20° degree in the wind tunnel. Experiment 2 followed after experiment 1 where the airfoil was added with slat at the leading edge of airfoil 5 different angle of attack 0°,5°,10°,15°,and 20° degree with 0°(upward) degree angle of slat. After done the experiment 2, experiment 3 was conduct it alike experiment 2 , the airfoil with slat at leading edge of airfoil just change the angle of slat with 30° (upward) degree angle of slat. Experiment 4 is same like experiment 2 and 3 just change the angle of slat with -30° (downward) degree angle of slat.

Experiment	parameter
1	Base case (airfoil only)
2	Airfoil with slat 0° angle of slat
3	Airfoil with slat +30°(upward) angle of slat
4	Airfoil with slat -30° angle(downward) of slat

TABLE 4.2.1 : LIST OF EXPERIMENT

4.2.1 Result for the base case (experiment 1)

Experiment 1, the base case is the origin of the problem which is involving the airfoil without any slat and flap. The experiment was conducted few times and the data are as below (Table 4.2.1)

Angle of attack (°)	Lift Force (N)			Drag Force (N)		
	Initial	Final	Difference	Initial	Final	Difference
0	-0.10	-0.10	0	-0.29	-0.29	0.00
5	-0.10	-0.20	-0.1	-0.29	-0.31	-0.02
10	-0.10	-0.30	-0.2	-0.30	-0.41	-0.11
15	-0.10	-0.50	-0.4	-0.30	-0.33	-0.03
20	-0.10	-0.70	-0.6	-0.29	-0.33	-0.04

Table 4.2.1 result for the base case

4.2.2 Result for the air foil with slat at leading edge with 0°angle of slat (experiment 2)

In experiment 2, the result for this experiment involving the modified airfoil when it is attached with leading edge slat. Just attached the slat with 5 different angle of attack of airfoil. Table below show the result of the experiment: Result for the test of 0° angle of slat.

Angle of slat (°)	Angle of attack (°)	Lift force (N)			Drag force (N)		
		Initial	Final	Actual	Initial	Final	Actual
0	0	0.00	-0.10	-0.10	-0.30	-0.25	0.05
	5	0.00	0.20	0.20	-0.26	-0.23	0.03
	10	0.00	0.40	0.40	-0.25	-0.21	0.04
	15	0.00	0.50	0.50	-0.25	-0.20	0.05
	20	0.00	0.60	0.60	-0.34	-0.19	0.15

Table 4.2.2: Result for the test of 0° angle of slat.

4.2.3 Result for the air foil with slat at leading edge with +30° angle of slat(experiment 3)

The Result of experiment 3 for the test of +30° (upward) angle of slat.

Angle of slat (°)	Angle of attack (°)	Lift force (N)			Drag force (N)		
		Initial	Final	Actual	Initial	Final	Actual
30 (upward)	0	-0.00	-0.10	0.10	-0.32	-0.24	0.08
	5	-0.10	-0.20	0.10	-0.28	-0.23	0.05
	10	-0.10	-0.30	0.20	-0.27	-0.24	0.03
	15	-0.10	-0.40	0.30	-0.27	-0.16	0.11
	20	-0.10	-0.70	0.60	-0.29	-0.18	0.11

Table 4.2.3: Result for the test of 30° angle of slat

4.2.4 Result for the air foil with slat at leading edge with -30° angle of slat (experiment 4)

The Result of experiment 4 for the test of -30° (downward) angle of slat.

Angle of slat (°)	Angle of attack (°)	Lift force (N)			Drag force (N)		
		Initial	Final	Actual	Initial	Final	Actual
-30 (downward)	0	-0.10	-0.10	0.00	-0.50	-0.38	0.12
	5	-0.10	-0.20	0.10	-0.45	-0.35	0.10
	10	-0.10	-0.30	0.20	-0.36	-0.33	0.03
	15	-0.10	-0.70	0.60	-0.35	-0.32	0.03
	20	-0.10	-1.00	0.90	-0.34	-0.32	0.02

Table 4.2.4: Result for the test of -30° (downward) angle of slat

4.3 Analysis

From the result of value of drag force and lift force obtained, the value of lift and drag coefficient can be calculated further using the mathematical equation for the drag and lift force. The analysis focus on the drag and lift coefficient. Value of drag coefficient, C_D can be calculated using the equation 1 as show below. We can see that the values of the difference between final and initial value of the lift force which represent the actual lift force acting on the airfoil are decreasing as it goes down the zero with negative value. Table 4.3.1 show the value that use in equation 1 to find drag and lift coefficient.

Symbol	**value**
Drag force , (F_D)	From the result
Lift force , (F_L)	From the result
Drag coefficient ,(C_D)	From the result
Lift coefficient, (C_L)	From the result
Density of air, (ρ)	1.1644 kg/m^3
Area of airfoil	0.0169m^2
Velocity of air,(v)	9.5m/s

Table 4.3.1 : data and symbol

$$C_D = \frac{2F_D}{\rho A V^2}$$ (Equation 1)

$$C_L = \frac{2F_L}{\rho A V^2}$$ (Equation 2)

4.3.1 Analysis of experiment 1

After get the result, the data from the result was convert to the line graph and the coefficient of lift and drag was calculate as show below:

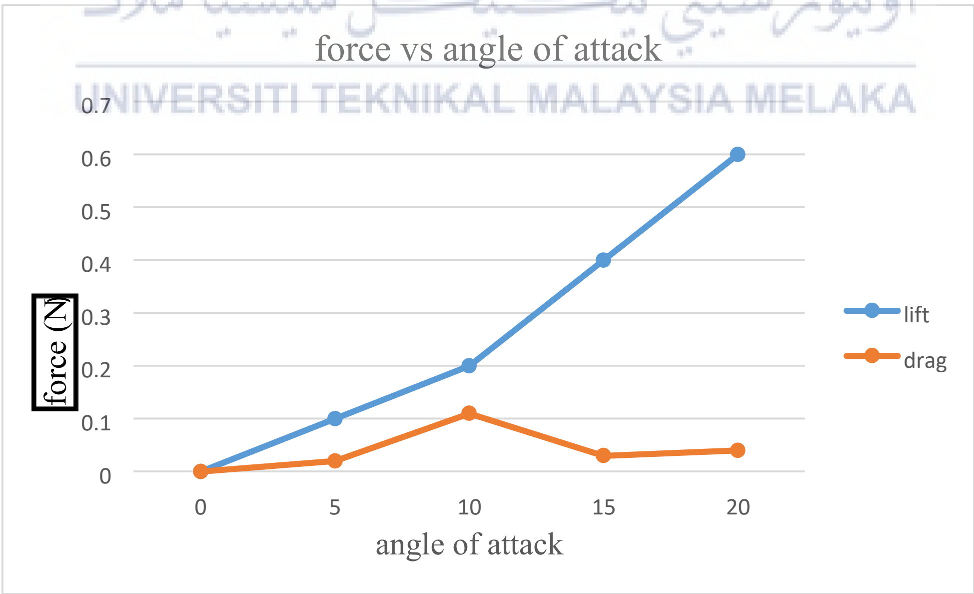

Chart 4.3.1.1 graph of force vs angle of attack

From the chart (4.3.1) we can see, the lift force rise higher than drag force. From the result in experiment 1, the lift and drag coefficient can be calculate by using equation

1. Table 4.3.1.1 show the drag and lift coefficient.

Angle of attack (°)	Lift		Drag	
	Lift Force (N)	Lift coefficient	Drag force (N)	Drag coefficient
0	0.00	0.000	0.00	0.000
5	0.10	0.113	0.02	0.023
10	0.20	0.225	0.11	0.124
15	0.40	0.450	0.03	0.034
20	0.60	0.676	0.04	0.045

Table 4.3.1.1: angle of attack with drag and lift coefficient

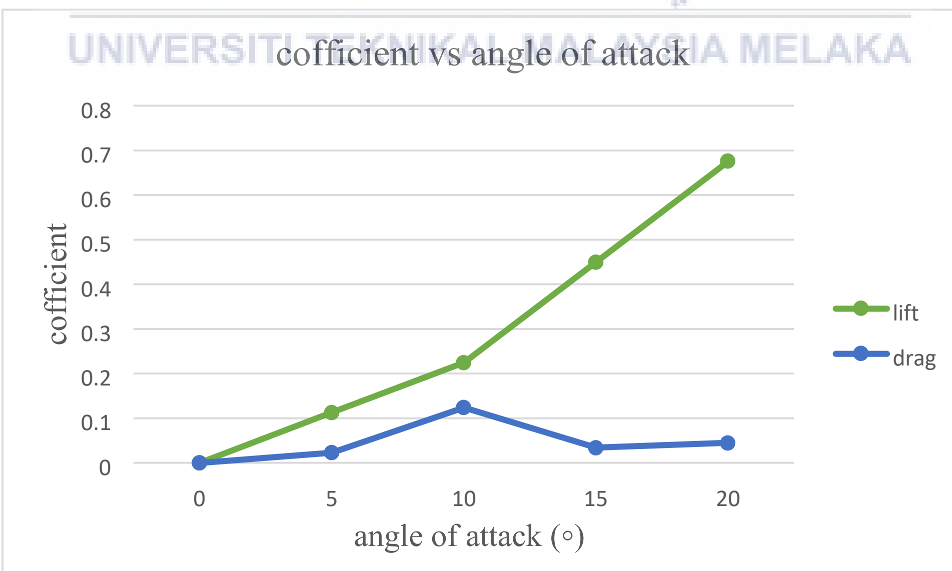

Chart 4.3.1.2: graph of coefficient vs angle of attack

From the chart 4.3.2.2, you can see there has not so many different with chart 4.3.1. We can see the lift coefficient rise directly proportional to the angle of attack. For the drag coefficient is fell slightly in the final quarter.

4.3.2 Analysis of experiment 2

In experiment 2 the airfoil is attached with a leading edge slat with angle of slat is 0°.

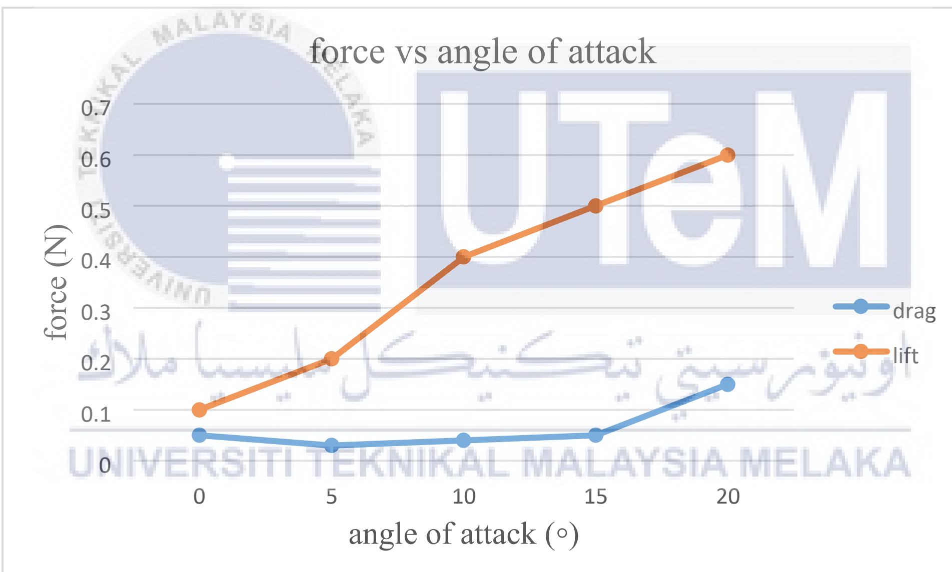

Chart 4.3.2.1: graph of force vs angle of attack

From the chart 4.3.2.1, the lift force at going to the max when the angle of attack is at 20°. While, the drag force is steady and sudden the force increase to 0.15 when the angle of attack is at 20°.

The next analysis is to find the lift and drag coefficient by doing some of calculation by using equation 1. Table 4.3.2.1 show the drag and lift coefficient.

Angle of attack (°)	Lift		Drag	
	Lift Force (N)	Lift coefficient	Drag force (N)	Drag coefficient
0	0.10	0.113	0.05	0.056
5	0.20	0.225	0.03	0.034
10	0.40	0.450	0.04	0.045
15	0.50	0.563	0.05	0.056
20	0.60	0.676	0.15	0169

Table 4.3.2.1: angle of attack with drag and lift coefficient

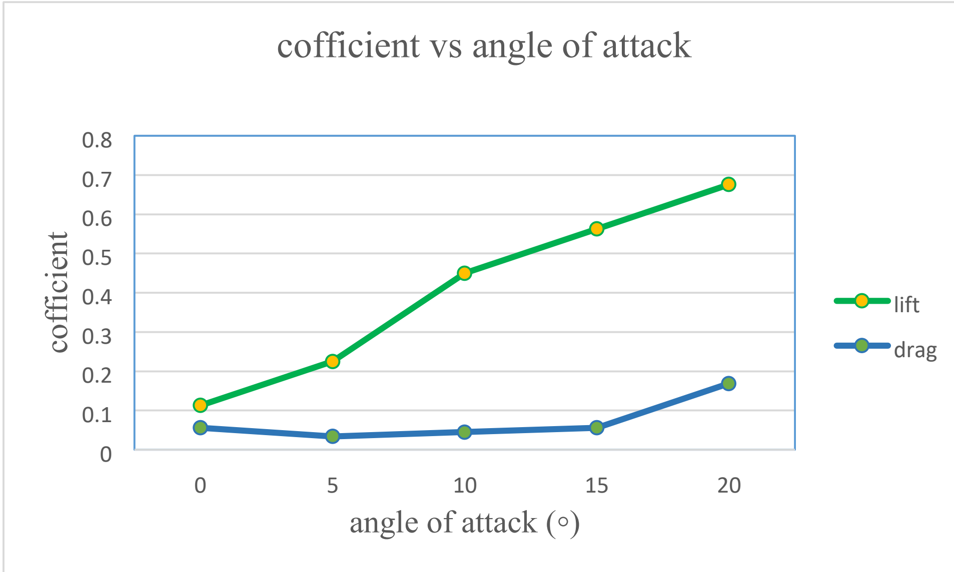

Chart 4.3.2.1: graph of coefficient vs angle of attack

From the graph above (4.3.2.1) the lift coefficient increase steadily from the beginning to the final. While, the drag coefficient same as before, the drag coefficient is steady and sudden the force increase to 0.16 when the angle of attack is at 20°.

4.3.3 Analysis of experiment 3

In experiment 2 the airfoil is attached with a leading edge slat with angle of slat is +30° (upward).

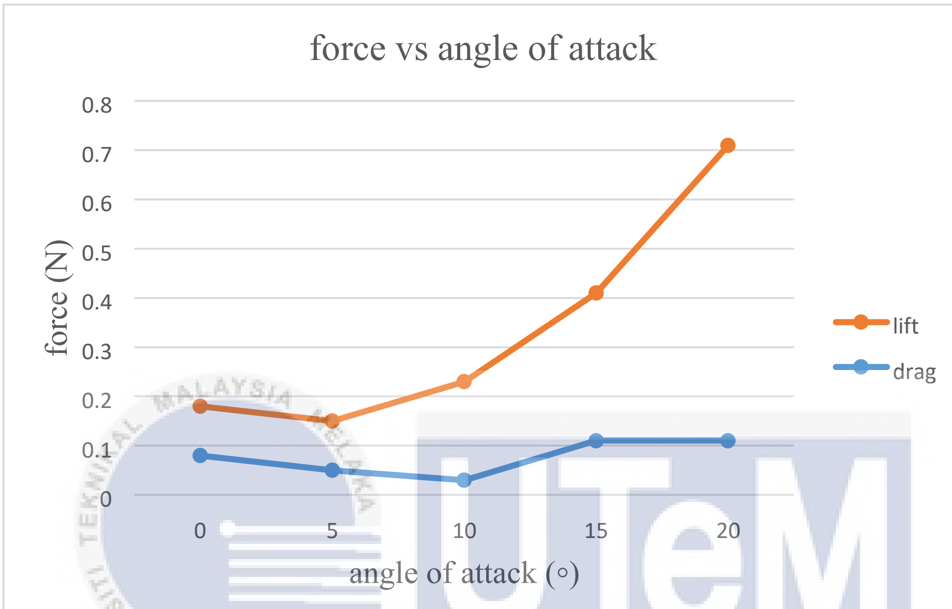

Chart 4.3.3.1: graph of force vs angle of attack

From the chart 4.3.3.1, the lift force rose from the angle of attack 5 ° to angle of attack 20 °.While, the drag force is steady and sudden the force increase to 0.11 when the angle of attack is at 15°.

The next analysis is to find the lift and drag coefficient by doing some of calculation by using equation 1. Table 4.3.3.1 show the drag and lift coefficient.

Angle of attack (°)	Lift		Drag	
	Lift Force (N)	Lift coefficient	Drag force (N)	Drag coefficient
0	0.10	0.113	0.05	0.056
5	0.20	0.225	0.03	0.034
10	0.40	0.450	0.04	0.045
15	0.50	0.563	0.05	0.056
20	0.60	0.676	0.15	0169

Table 4.3.3.1: angle of attack with drag and lift coefficient

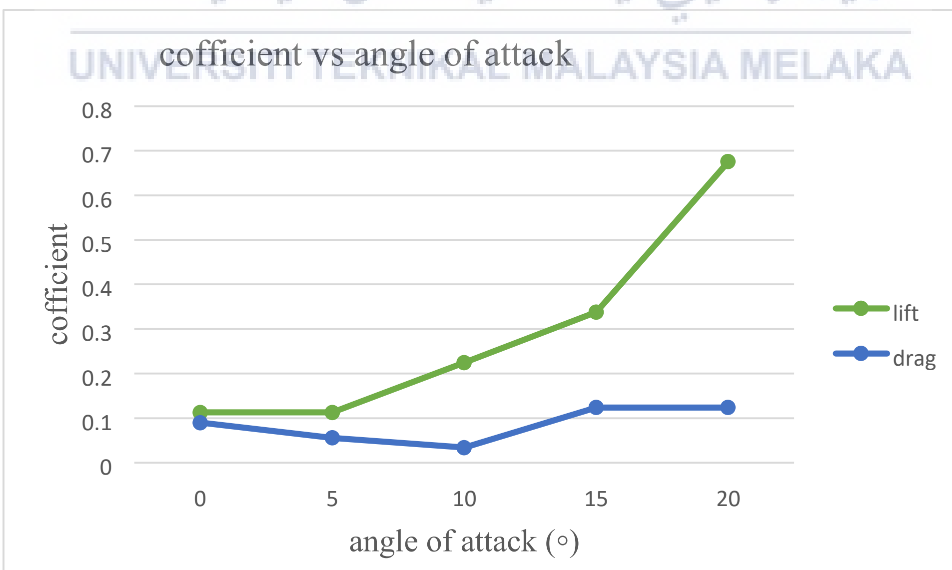

Chart 4.3.3.1: graph of coefficient vs angle of attack

From the graph above (4.3.3.1) the lift coefficient increase steadily from the angle of attack at 5 ° to 20 °. While, the drag coefficient same as before, the drag coefficient is steady and sudden the force increase to 0.16 when the angle of attack is at 15°.

4.3.4 Analysis of experiment 4

In experiment 2 the airfoil is attached with a leading edge slat with angle of slat is -30° (downward).

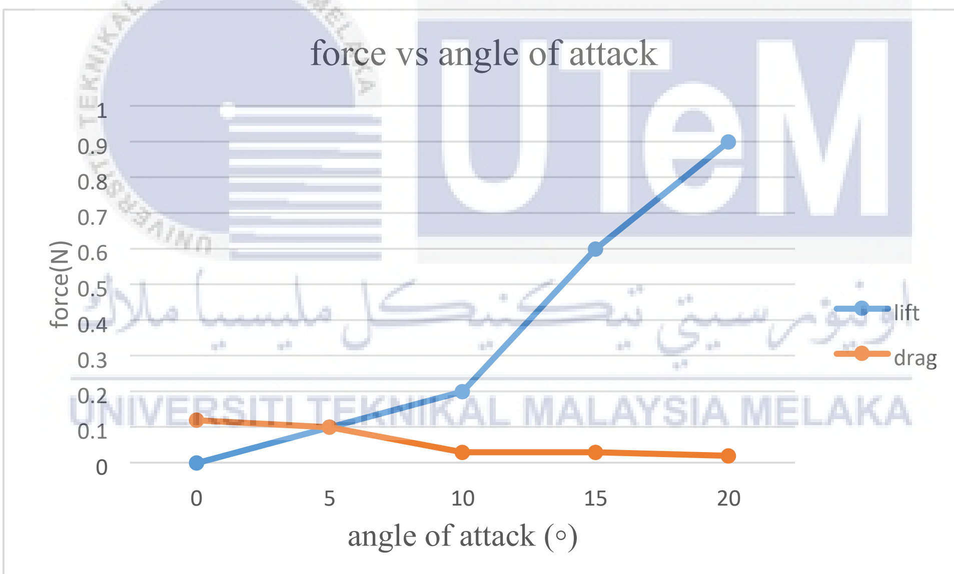

Chart 4.3.4.1: graph of force vs angle of attack

From the chart 4.3.4.1, the lift force slightly increase at the angle of attack 10 °. While, the drag force is steady and sudden the force increase to 0.11 when the angle of attack is at 15°.while the drag force still low from the beginning until final.

The next analysis is to find the lift and drag coefficient by doing some of calculation by using equation 1. Table 4.3.4.1 show the drag and lift coefficient.

Angle of attack (°)	Lift		Drag	
	Lift Force (N)	Lift coefficient	Drag force (N)	Drag coefficient
0	0.00	0.000	0.05	0.056
5	0.10	0.113	0.03	0.034
10	0.20	0.225	0.04	0.045
15	0.60	0.676	0.05	0.056
20	0.90	1.014	0.15	0169

Table 4.3.4.1: angle of attack with drag and lift coefficient

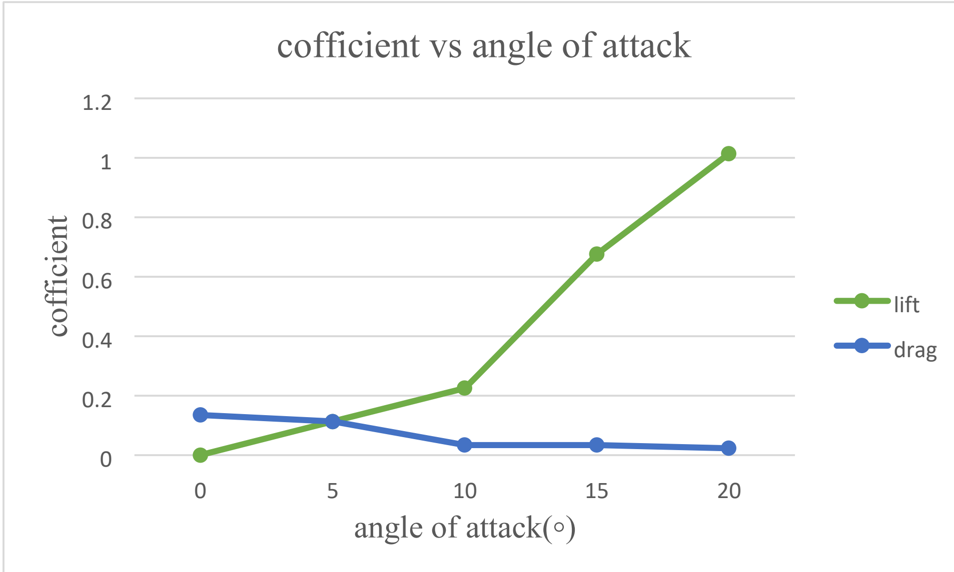

Chart 4.3.4.1: graph of coefficient vs angle of attack

From the graph above (4.3.4.1) the lift coefficient increase steadily from the angle of attack at 5 ° to 20 °. Meanwhile, as we can see from the graph, the drag coefficient still low from the beginning until final.

4.3.5 Experiment compare

In this section, is to compare between experiment 1,2,3 and 4. This section are compare the different of lift coefficient of all experiment. Chart 4.3.5.1 show the graph of lift coefficient vs angle of attack of all experiment. Meanwhile, chart 4.3.5.2 show graph of the drag coefficient vs angle of attack of all experiment

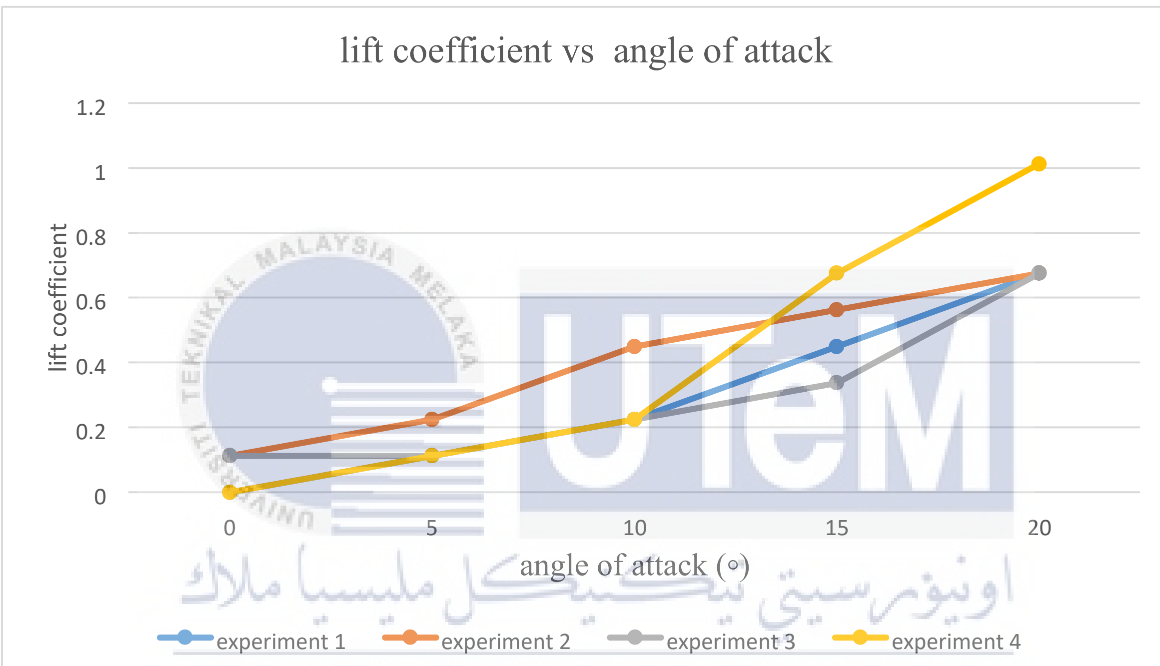

Chart 4.3.5.1: graph lift coefficient vs angle of attack

As we can see, experiment 4 (-30° angle of slat) get the higher of lift coefficient at 20° angle of attack between the other experiment. While, experiment 2 (0° angle of slat) steadily increase from the beginning to 20° angle of attack. Experiment 1,2 and 3 get the same value of lift coefficient at the angle of attack 5° and 10°.

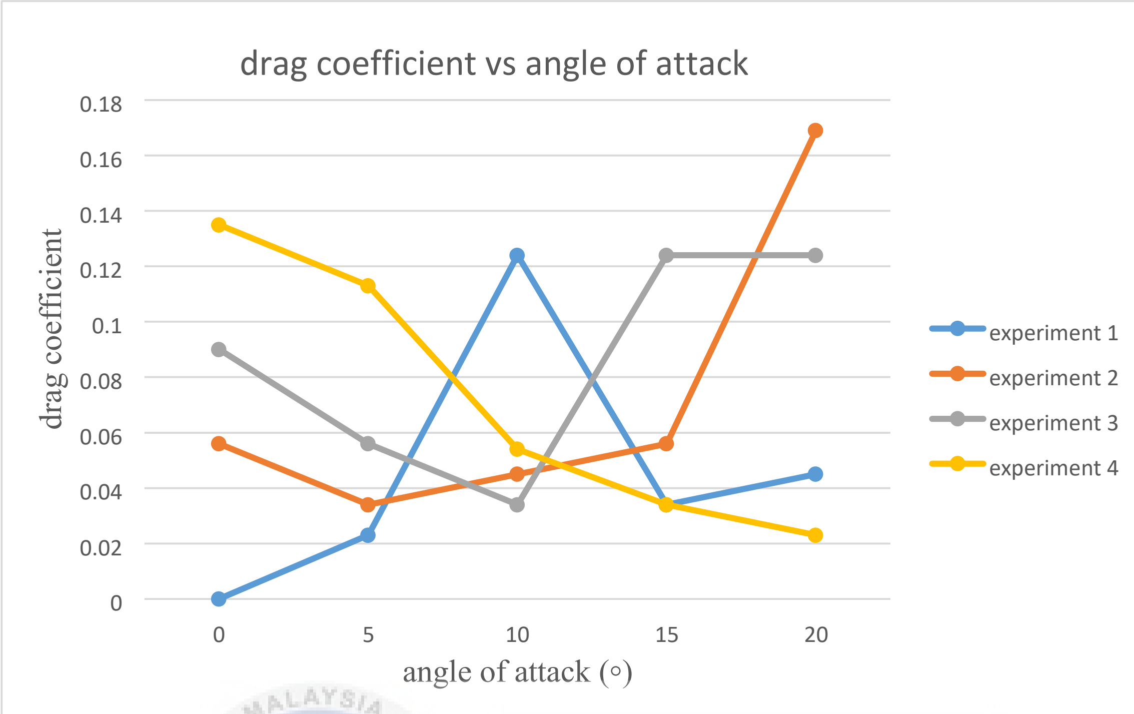

Chart 4.3.5.2: graph drag coefficient vs angle of attack

For the experiment 2, the drag coefficient get the highest of value at the 20° angle of slat. The drag coefficient for experiment 4 is the highest is value at 0° angle of slat. for experiment 1, the drag coefficient increase immediately from 0.023 at angle of attack 5° to 0.124 at angle of attack 10°. For experiment 3, the drag coefficient remain same at angle of attack 15° to 20°.

CHAPTER 5

CONCLUSION AND RECOMMENDATION

The analysis of slat on airfoil should be emphasized as the application of airplane is greatly increase nowadays. The function and efficiency of slat on airfoil due to increase lift force is the main characteristic or parameter to control the life and efficiency of those aerodynamic object especially for aircraft.

The lift and drag force of airfoil has been determined by using 4 different experiment. From the experiment, the result of effect of slat to aerodynamic performance of airfoil have being compare with airfoil without slat. based on comparison for all experiment which are conducted at different angle of attack, 0°,5°,10°,15°,20° and 3 different angle of slat show the positive result.

From the results and analysis, we can see clearly there have a different airfoil with slat and airfoil without slat, which experiment 4 (airfoil with angle of slat -30°) because this experiment get the highest in lift coefficient and lowest in drag coefficient with 20° angle of attack. On the other hand, while producing high lift coefficient, this arrangement were also producing small value of drag coefficient.

For future works, the effect of slat to aerodynamic performance of airfoil can be improved by manipulating the parameter of airfoil such as the angle of slat and the angle of attack of airfoil. Other than that, the material of airfoil can also be manipulate to increase the strength of airfoil.

Overall, the result from the work indicate slat on the airfoil has a big impact to the aerodynamic performance of airfoil and show the positive results. For airfoil with slat show the better performance compare to airfoil without slat.

REFERENCE

1. CarlosC.Pagani n, DanielS.Souza 1, MarcelloA.F.Medeiros Department of Aeronautics Engineering, São C arlos Engineering School, University of São Paulo, 13566-590 São Carlos, Brazil

2. W.L. Siauw a , b , , UPR CNRS 3346, Universities Poitiers ISAE-ENSMA, 11 Boulevard Marie et Pierre Curie, 86962 Futuroscope Chasseneuil Cedex, France b DSO Nat. Lab., 12 Science Park Drive, Singapore 1 18225 Malaysia

3. S.R. Maddah a, T. Gough a, B. Pierscionek b, H.H. Bruun a,* a Department of Mechanical and Medical Engineering , University o f Bradford,
   Bradford BD7 1DP, UK Department of Biomedical Sciences, University of Bradford, Bradford BD7 1DP, UK

4. D.S.Souzaa,*, D.Rodrígueza,b, L.G.C.Simõesa,c, M.A.F.Medeirosa
   A *Universidade de São Paulo, Rua João Dagnone 1100, 13563-120 , São Carlos,*
   Brazil Universidad Politécnica de Madrid, Plaza del Cardenal Cisneros 3, 28040,
   Madrid, Spain c*EMBRAER, Av. Brigadeiro Faria Lima 2170, 12227-901, São José dos Campos, Brazil*

5. Huan Pang * , Tianxiang Yu, Bifeng Song
   School of Aeronautics, Northwestern Polytechnical University, P.O. Box 120, No. 127, West Youyi Road, Beilin, Xi'an City, Shaanxi Province, PR China

6. [2D.G. Crighton,Airframenoise, Aeroacous. tics FlightVeh.:TheoryPract. 1 (1991)391–447

7. Y.P.Guo,M. . C.Joshi,N. oisecharacteristicsofaircrafthighliftsystems, J. Aircr. 1(7)(2003)1247–1256.

8. [Y.P.Guo,K.J.Yamamot. o,R.W.Stoker,Component-basedempiricalmodelforhighliftsystemnoiseprediction, J. Aircr. 40 (5)(2003)914–922.

9. B.Storms,J.Hayes,J.Ross,Aeroacousticmeasurementsofslatnoiseonathree-

10. M.M.Choudhari,D.P.Lockard,M.G.Macaraeg,B.A.Singer,C.L.Streett,G.R.Neubert,R.W.S toker,J.R.Underbrink,M.E.Berkman,M.R.Khorrami,

11. W.Dobrzynski,K.Nagakura,B.Gehlhar,A.Buschbaum,Airframenoisestudiesonwingswithd eployedhigh-liftdevices,AIAAPaper98-2337,1998.

12. W.Dobrzynski,M.Pott-Pollenske,Slatnoisesourcestudiesforfarfieldnoise. prediction,AIAAPaper2001-2158,2001.

13. Agarwal,Anurag,Morris,J. .Philip,Broadbandnoisefromtheunsteadyflowinaslatcove,AIAAPaper2004-854,2004.

14. A.Kolb,P.Faulhaber,R.Drobietz,M.Grunewald,Aeroaco . usticwindtunnelmeasurementsona2Dhigh-liftconfiguration,AIAAPaper2007-3447, 2007.

15. E.Manoha,M.Terracol,B.Lemoine,L.I.Griffon,L . .T.Garrec,SlatnoisemeasurementandnumericalpredictionintheVALIANTprogramme,AIA APaper 2012-2100,2012.

16. KyleA.Pascioni,LouisN.Cattafesta,MeelanM.Choudhari,Anexperimentalinvestigationofth e30P30Nmulti-elementhigh-liftairfoil,AIAA Paper 2014-3062,2014.

17.]M.Murayama,K. .Nakakita,K.Yamamoto,H.Ura,Y.Ito,M.Choudhari,Experimentalstudyonslatnoisefrom30 P30Nthree-elementhigh-liftairfoil at JAXA hardwalllowspeedwindtunnel,in:AIAAAviationandAeronau. ticsForumandExposition(AVIATION2014);16–20 June2014,Atlanta,GA, UnitedStates2014–2080, 2014.

18. T.Imamura,H.Ura,Y.Yokokawa,K.Yamamoto,Afar-fieldnoiseandnear-fieldunsteadinesso. fasimplifiedhigh-lift-configurationmodel(slat), in: Proceedings ofthe47thAIAAAerospaceSciencesMeetingIncludingTheNewHorizonsForumandAerospa ceExposition,5–8 January2. 009,Orlando, Florida 2009–1239,2009. [15]

19. Bart A.Singer,DavidP.Lockard,Ken. nethS.Brentner,Computationalaeroacousticanalys. isofslattrailing-edgeflow, AIAA J. 38 (9)(2000)1558–1564.

20. C.K.W.Tam,N.Pastouc. henko,G.
apTones:AComponentofAirframeNoise,AIAAPaper2000-0606,2000.
[18]K.Paschal,L.Jenkins,C. . ao,Unsteadyslat-wakec. haracteristicsofahigh-liftconfigur. ation,AIAA. Paper2000-0139,2000.

21. K.Takeda,X.Zha.ng,G.B.Ashcroft,P.A.Nelson,Unsteadyaerodynamicsofflapcoveflowinahigh-liftdeviceconfiguration,AIAAPaper2001-0707,2001.

22. M.Roger,S.Perennes, . Low-frequencynoisesourcesintwo-dimensionalhigh-liftdevice. AIAAPaper2000-1972,2000. [21] S. Hein,T.Hohage,W.Koch,J.Schöberl,A. cousticresonancesinah. igh-liftconfiguration, J. FluidMech. 585 (2007)179–202